




# Evolution of size distribution of Si nanoparticles produced by pulsed laser ablation in water

A. Krivonosov<sup>1</sup> · D. Zuev<sup>1</sup> · S. Kaputkina<sup>2</sup> · V. Mikhailovskii<sup>2</sup> · E. Egorova<sup>1</sup>  · E. Ageev<sup>1</sup> · G. Odintsova<sup>1</sup>

Received: 3 October 2019 / Accepted: 15 February 2020 / Published online: 29 February 2020  
© Springer Science+Business Media, LLC, part of Springer Nature 2020

## Abstract

In this work, we study ablation of silicon in distilled water under the action of laser pulses with nanosecond duration. The size distribution of produced particles depends on the laser processing parameters and therefore can be modified by the varying distance between laser pulses, laser fluence or pulse duration. The properties of fabricated nanostructures are investigated by scanning electron microscopy to acquire statistical information on nanoparticle sizes. These results can be promising for dielectric nanophotonics, photovoltaics or cancer treatment where relatively large spherical silicon particles are necessary.

**Keywords** Nanoparticles · Silicon nanoparticles · Laser ablation · Size dependence · Fracture

## 1 Introduction

Quantum confinement effect provides a dramatic change in the properties of bulk material compared to nanoparticles (NPs). This change can be manifested in NPs optical, chemical, or other characteristics, motivating a strong demand for various types of nanomaterials and therefore, the fast development of their fabrication techniques.

Silicon is one of the most widespread semiconductor materials in the world, commonly used in the current manufacture of electronic components. Decrease of Si crystal size down to nanoscale results in a significant change of electronic energy bands luminescent properties in the visible and near-infrared (IR) (Takagi et al. 1990) and enhanced absorption in the ultraviolet, visible and IR (Her et al. 1998; Wu et al. 2002). These properties open up numerous

---

This article is part of the Topical Collection on Fundamentals of Laser Assisted Micro- & Nanotechnologies.

---

Guest edited by Tigran Vartanyan, Vadim Veiko, Andrey Belikov and Eugene Avrutin.

---

✉ E. Egorova  
elena1998959@gmail.com

<sup>1</sup> ITMO University, 49 Kronverksky Pr., St. Petersburg, Russia 197101

<sup>2</sup> St. Petersburg State University, 7/9 Universitetskaya nab, St. Petersburg, Russia 199034

promising applications in photonics (optical nanoantennas (Krasnok et al. 2013), detectors (Gonzalez and Veinot 2016) and many others), photovoltaics (Priolo et al. 2014; Wippermann et al. 2016), biology and medicine [drug delivery (Salonen et al. 2008), fluorophores (Gu et al. 2013) and photodynamic therapy (Kovalev and Fujii 2005; Timoshenko et al. 2006)].

In general silicon nanomaterials can be fabricated by chemical, physical, physicochemical, and electrochemical methods [one can find a recent review in (Kabashin et al. 2019)]. Recently laser-assisted methods of Si NPs formation called great attention due to provided chemical purity and ability to control the size, phase state, and morphology of produced nanomaterials. Among them pulsed laser ablation in liquids (PLAL) (Dolgaev et al. 2002; Fojtik and Henglein 1993) is a rather simple method of synthesis (there is no complicated vacuum or chemical equipment) yielding in production of NPs colloidal solution, which can be easily stored, transported or used to develop various functional surfaces (Thompson et al. 2013).

Nanosecond PLAL (Abderrafi et al. 2011) is an attractive method, since strong competitiveness and reliability of available fiber-based laser sources. Generated NPs have a wide distribution of sizes, which can be further tailored through laser-induced fragmentation (Eidelman et al. 2017) or size-selectively optically printed from colloid (Zaza et al. 2019) to fit a particular application.

Very recently, spherical Si nanoparticles with sizes of a few hundred nanometers (100–400 nm) attracted a great interest due to excitation of strong electric and magnetic dipole resonances providing a unique optical response in the visible and near IR ranges (Krasnok et al. 2013). For example, silicon particles with diameter 80–160 nm was proposed for NP antireflective coatings (Baryshnikova et al. 2016). Enhanced emission extraction and selective excitation of NV centers were demonstrated with the silicon nanoparticles with sizes of a few hundred nanometers (Krasnok et al. 2015). Oligomers from silicon nanospheres with an average size of about 100 nm were used to experimentally demonstrate magnetically induced transparency (Yan et al. 2015).

Applied to photovoltaics and energy storage sub-10 nm silicon NPs can enhance conversion efficiency of commercial solar cells (Rasouli et al. 2017); active Si NPs (100–400 nm) material sealed in pores of 3D microporous current collector by graphene layers significantly improves a cycling stability of Li-Ion battery (Shelke et al. 2017). Si particles with sizes in the range from ~40 to ~250 nm in diameter NPs can be of direct interest for solar water heating and vaporization (Ishii et al. 2016).

In medical applications, the laser-ablated Si NPs with a mean size of 25–30 nm in diameter were used to improve the efficiency of radio frequency-based treatment of cancer (Tamarov et al. 2014). PEG-coated laser-synthesized Si NPs (mean size about 25 nm) were conjugated with radioactive  $^{188}\text{Re}$  and used as suitable carriers at nuclear therapy (Petriev et al. 2019).

However, most papers in the formation of Si NPs by nanosecond PLAL devoted to NPs generation with particular size (Rawat et al. 2018; Ulusoy Ghobadi et al. 2016; Vaccaro et al. 2014) and therefore did not consider size dependence on laser processing parameters. Here for nanosecond PLAL, we study the effect of laser fluence, pulse duration and scanning strategy on size of formed Si NPs.

## 2 Materials and methods

Commercially available machine (Minimarker 2) on the base of ytterbium pulsed fiber laser ( $\lambda = 1.06 \mu\text{m}$ ,  $\tau = 4\text{--}200 \text{ ns}$ ,  $f = 10\text{--}99 \text{ kHz}$ , maximum average power  $P_{\text{aver}} = -20 \text{ W}$ ) was used. The laser spot with a focal diameter of  $d_0 = 50 \mu\text{m}$  was moved

over the sample surface with a velocity  $V_{sc}$  from 1 to 8000 mm/s. An experimental design is presented in Fig. 1.

The silicon wafer with sizes of  $7 \times 7 \times 0.25$  mm was used as the target. Samples were ultrasonically washed in distilled water and acetone in sequence. Then cleaned substrate was placed to contamination-free Petrie dish filled with 2 ml of distilled water, where nanosecond PLAL took place. Finally, 50  $\mu$ l of obtained colloidal solution was dropped on silicon substrate dried out under normal conditions for subsequent studies.

The resulting NPs were investigated in an Auriga (Carl Zeiss) scanning electron microscope (SEM) operating at 20 kV. SEM images were analyzed with an open-source software ImageJ (Schneider et al. 2012) to acquire statistical information on NPs sizes.

Laser particle size analyzer SZ100 (Horiba Jobin–Yvon) was used to measure the zeta-potential of colloidal solutions.

### 3 Results and discussion

#### 3.1 Effect of scanning strategy on NPs size

PLAL process is accompanied with cavitation bubble appearance (Tsuji et al. 2004), in the case of nanosecond duration of laser pulses bubble size and lifetime can be up to 200  $\mu$ m and 100–200  $\mu$ s (De Giacomo et al. 2013; Lam et al. 2016), that could have a substantial impact on NPs generation. Three typical cases can be selected: the distance between consecutive laser pulses is higher than cavitation bubble size, laser pulses come one after another immediately (0% overlapping), and 50% pulse overlapping (Fig. 2). For all tests here, pulse duration is 50 ns and fluence is 10 J/cm<sup>2</sup>.

For short distance between pulses or their overlapping laser radiation is partially blocked by growing cavitation bubble, thereby providing additional heating, that results in an enhancement of agglomeration processes in the bubble volume. At the same time, the heating of silicon target decreases due to partial loss of laser power, which has a negative impact on NPs concentration in the solution.

Therefore, the optimal scanning pattern for the generation of NPs with the highest concentration and uniformity of size distribution is that supporting the 350  $\mu$ m distance between laser pulses. This pattern is used at all experiments stated below.

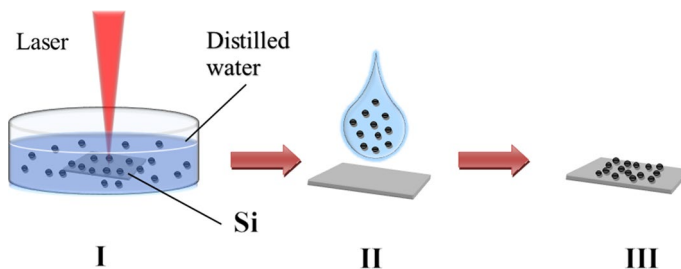


**Fig. 1** A schematic course of the experiment: **I** ablation of Si target by nanosecond laser pulses in distilled water, **II** drop deposition of obtained colloidal solution on silicon substrate, **III** natural drying and preparation for SEM studies

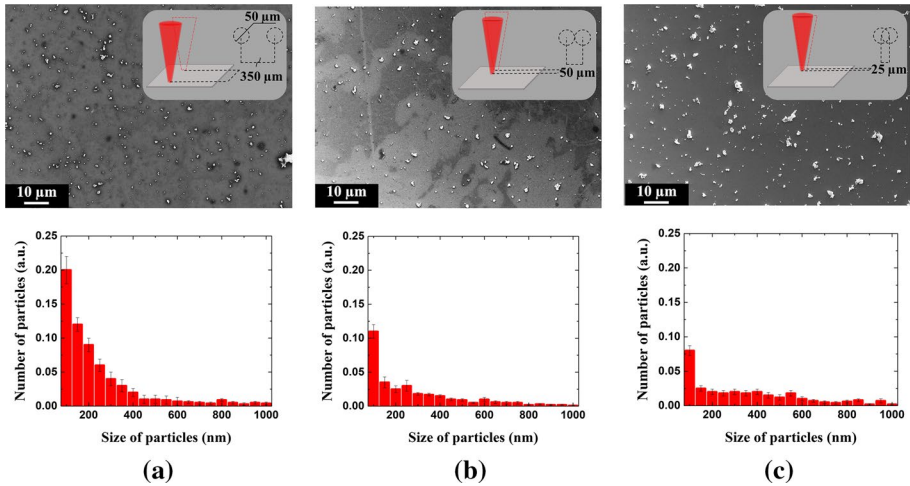


**Fig. 2** SEM images (first row) and size distribution histograms (second row) of Si NPs formed by PLA in water for different distances between laser pulses (*overlapping*): **a** 350 μm (0%), **b** 50 μm (0%) and **c** 25 μm (50%)

### 3.2 Effect of laser fluence (in the range 5–15 J/cm<sup>2</sup>) on NPs size

Silicon ablation threshold for 50 ns laser pulses at 1064 nm was experimentally found to be equal to 2 J/cm<sup>2</sup>. Therefore, to ensure intense ablation of a silicon target, the lowest used fluence is 5 J/cm<sup>2</sup>, while upper boundary (15 J/cm<sup>2</sup>) comes from a processing limit of available laser source. Figure 3 presents obtained results. One can see that fluence growth gives considerable increase in NPs concentration, while size distribution is not uniform—both large and small particles can be found. Probably it comes from an enlargement of ablated silicon as the fluence increases.

### 3.3 Effect of laser pulse duration (in the range 50–200 ns on NPs size

To investigate the effect of laser pulse duration on the size of formed NPs all PLAL experiments in this section was made at the fluence of 10 J/cm<sup>2</sup> (Fig. 4).

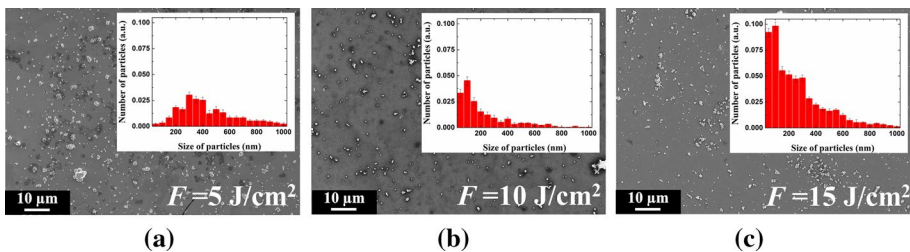


**Fig. 3** SEM images and size distribution histograms (insets) of Si NPs formed by PLA in the water at different fluences: **a** 5 J/cm<sup>2</sup>, **b** 10 J/cm<sup>2</sup> and **c** 15 J/cm<sup>2</sup>

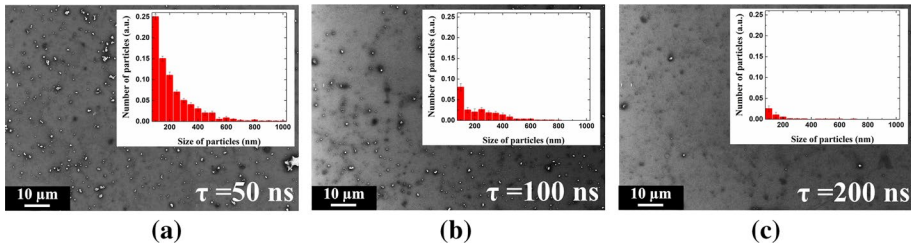


**Fig. 4** SEM images and size distribution histograms (insets) of Si NPs formed by PLA in the water at different durations of laser pulses: **a** 50 ns, **b** 100 ns and **c** 200 ns

**Table 1** Effect of laser processing parameters on Si NPs size at PLA in water

	Size distribution (nm)
Distance between laser pulses ( $\mu\text{m}$ )	
350	$204 \pm 33$
50	$375 \pm 57$
25	$573 \pm 75$
Laser fluence ( $\text{J}/\text{cm}^2$ )	
5	$226 \pm 40$
10	$164 \pm 21$
15	$500 \pm 117$
Pulse duration (ns)	
50	$210 \pm 45$
100	$132 \pm 32$
200	$126 \pm 10$

In the case of 50 ns laser pulses, silicon reaches higher temperatures than for 100 ns and 200 ns pulses due to faster heating. Therefore, it longer resides in a liquid state after the cavitation bubble collapse, and consequently there is higher probability of agglomeration processes. Potentially, it could provide a quantity reduction for large particles with an increase in laser pulse duration.

To analyze the stability of colloidal solutions, zeta-potential measurements were performed. The typical value is found to be  $-60$  mV, which is indicative of high solution stability and a low tendency for agglomeration. Table 1 summarizes the data of experimental findings.

### 4 Summary

In this work, Si NPs produced by nanosecond PLA in distilled water was investigated. This process allows generation of NPs with a wide distribution of sizes, which can be modified to some extent by altering key laser processing parameters—the distance between laser pulses, laser fluence, and pulse duration.

These results represent the initial step to the fabrication of spherical silicon particles for the benefit of such rapidly developing areas as dielectric nanophotonics, photovoltaics or cancer treatment where relatively large spherical silicon particles are necessary.

**Acknowledgements** The study is funded by a grant Russian Science Foundation (project № 19-79-10208). SEM studies were done on the base of the Interdisciplinary Resource Center for Nanotechnology, Research Park, St. Petersburg State University. Zeta-potential measurements were performed at the Center for Optical and Laser Materials Research, Research Park, St. Petersburg State University.

## References

- Abderrafi, K., García Calzada, R., Gongalsky, M.B., Suárez, I., Abarques, R., Chirvony, V.S., Timoshenko, V.Y., Ibáñez, R., Martínez-Pastor, J.P.: Silicon nanocrystals produced by nanosecond laser ablation in an organic liquid. *J. Phys. Chem. C* **115**, 5147–5151 (2011). <https://doi.org/10.1021/jp109400v>
- Baryshnikova, K.V., Petrov, M.I., Babicheva, V.E., Belov, P.A.: Plasmonic and silicon spherical nanoparticle antireflective coatings. *Sci. Rep.* **6**, 22136 (2016)
- De Giacomo, A., Dell’Aglia, M., Santagata, A., Gaudiuso, R., De Pascale, O., Wagener, P., Messina, G.C., Compagnini, G., Barcikowski, S.: Cavitation dynamics of laser ablation of bulk and wire-shaped metals in water during nanoparticles production. *Phys. Chem. Chem. Phys.* **15**, 3083–3092 (2013)
- Dolgaev, S.I., Simakin, A.V., Voronov, V.V., Shafeev, G.A., Bozon-Verduraz, F.: Nanoparticles produced by laser ablation of solids in liquid environment. *Appl. Surf. Sci.* **186**, 546–551 (2002)
- Eidelman, K., Gudkov, D., Segbefia, O., Ageev, E., Krivososov, A., Matuhina, A.: Evolution of size distribution and structure of Si and SiO<sub>2</sub> nanoparticles: laser-assisted formation and fragmentation. *J. Phys: Conf. Ser.* **917**, 032027 (2017). <https://doi.org/10.1088/1742-6596/917/3/032027>
- Fojtik, A., Henglein, A.: Laser ablation of films and suspended particles in a solvent: formation of cluster and colloid solutions. *Berichte der Bunsen-Gesellschaft* **97**, 252–254 (1993)
- Gonzalez, C.M., Veinot, J.G.C.: Silicon nanocrystals for the development of sensing platforms. *J. Mater. Chem. C* **4**, 4836–4846 (2016)
- Gu, L., Hall, D.J., Qin, Z., Anglin, E., Joo, J., Mooney, D.J., Howell, S.B., Sailor, M.J.: In vivo time-gated fluorescence imaging with biodegradable luminescent porous silicon nanoparticles. *Nat. Commun.* **4**, 2326 (2013)
- Her, T.-H., Finlay, R.J., Wu, C., Deliwala, S., Mazur, E.: Microstructuring of silicon with femtosecond laser pulses. *Appl. Phys. Lett.* **73**, 1673–1675 (1998)
- Ishii, S., Sugavaneshwar, R.P., Chen, K., Dao, T.D., Nagao, T.: Solar water heating and vaporization with silicon nanoparticles at mie resonances. *Opt. Mater. Express.* **6**, 640–648 (2016). <https://doi.org/10.1364/OME.6.000640>
- Kabashin, A.V., Singh, A., Swihart, M.T., Zvestovskaya, I.N., Prasad, P.N.: Laser processed nanosilicon: a multifunctional nanomaterial for energy and health care. *ACS Nano* **13**, 9841–9867 (2019)
- Kovalev, D., Fujii, M.: Silicon nanocrystals: photosensitizers for oxygen molecules. *Adv. Mater.* **17**, 2531–2544 (2005)
- Krasnok, A.E., Maksymov, I.S., Denisyuk, A.I., Belov, P.A., Miroshnichenko, A.E., Simovski, C.R., Kivshar, Y.S.: Optical nanoantennas. *Phys. Usp.* **56**, 539–564 (2013). <https://doi.org/10.3367/UFNe.0183.201306a.0561>
- Krasnok, A.E., Maloshtan, A., Chigrin, D.N., Kivshar, Y.S., Belov, P.A.: Enhanced emission extraction and selective excitation of NV centers with all-dielectric nanoantennas. *Laser Photon. Rev.* **9**, 385–391 (2015)
- Lam, J., Lombard, J., Dujardin, C., Ledoux, G., Merabia, S., Amans, D.: Dynamical study of bubble expansion following laser ablation in liquids. *Appl. Phys. Lett.* **108**, 74104 (2016)
- Petriev, V.M., Tischenko, V.K., Mikhailovskaya, A.A., Popov, A.A., Tselikov, G., Zelepukin, I., Deyev, S.M., Kaprin, A.D., Ivanov, S., Timoshenko, V.Y.: others: Nuclear nanomedicine using Si nanoparticles as safe and effective carriers of 188 Re radionuclide for cancer therapy. *Sci. Rep.* **9**, 2017 (2019)
- Priolo, F., Gregorkiewicz, T., Galli, M., Krauss, T.F.: Silicon nanostructures for photonics and photovoltaics. *Nat. Nanotechnol.* **9**, 19–32 (2014). <https://doi.org/10.1038/nnano.2013.271>
- Rasouli, H.R., Ghobadi, A., Ghobadi, T.G.U., Ates, H., Topalli, K., Okyay, A.K.: Nanosecond pulsed laser ablated sub-10 nm silicon nanoparticles for improving photovoltaic conversion efficiency of commercial solar cells. *J. Opt.* **19**, 105902 (2017)
- Rawat, R., Tiwari, A., Vendamani, V.S., Pathak, A.P., Rao, S.V., Tripathi, A.: Synthesis of Si/SiO<sub>2</sub> nanoparticles using nanosecond laser ablation of silicate-rich garnet in water. *Opt. Mater. (Amst)* **75**, 350–356 (2018)
- Salonen, J., Kaukonen, A.M., Hirvonen, J., Lehto, V.-P.: Mesoporous silicon in drug delivery applications. *J. Pharm. Sci.* **97**, 632–653 (2008)

- Schneider, C.A., Rasband, W.S., Eliceiri, K.W.: NIH Image to ImageJ: 25 years of image analysis. *Nat. Methods* **9**, 671–675 (2012)
- Shelke, M.V., Gullapalli, H., Kalaga, K., Rodrigues, M.-T.F., Devarapalli, R.R., Vajtai, R., Ajayan, P.M.: Facile synthesis of 3D anode assembly with Si nanoparticles sealed in highly pure few layer graphene deposited on porous current collector for long life Li-ion battery. *Adv. Mater. Interfaces* **4**, 1601043 (2017)
- Takagi, H., Ogawa, H., Yamazaki, Y., Ishizaki, A., Nakagiri, T.: Quantum size effects on photoluminescence in ultrafine Si particles. *Appl. Phys. Lett.* **56**, 2379–2380 (1990). <https://doi.org/10.1063/1.102921>
- Tamarov, K.P., Osminkina, L.A., Zinovyev, S.V., Maximova, K.A., Kargina, J.V., Gongalsky, M.B., Ryabchikov, Y., Al-Kattan, A., Sviridov, A.P., Sentis, M., et al.: Radio frequency radiation-induced hyperthermia using Si nanoparticle-based sensitizers for mild cancer therapy. *Sci. Rep.* **4**, 7034 (2014)
- Thompson, C.S., Fleming, R.A., Zou, M.: Transparent self-cleaning and antifogging silica nanoparticle films. *Sol. Energy Mater. Sol. Cells* **115**, 108–113 (2013)
- Timoshenko, V.Y., Kudryavtsev, A.A., Osminkina, L., Vorontsov, A.S., Ryabchikov, Y.V., Belogorokhov, I.A., Kovalev, D., Kashkarov, P.K.: Silicon nanocrystals as photosensitizers of active oxygen for biomedical applications. *JETP Lett.* **83**, 423–426 (2006)
- Tsuji, T., Tsuboi, Y., Kitamura, N., Tsuji, M.: Microsecond-resolved imaging of laser ablation at solid–liquid interface: investigation of formation process of nano-size metal colloids. *Appl. Surf. Sci.* **229**, 365–371 (2004)
- Ulusoy Ghobadi, T.G., Ghobadi, A., Okyay, T., Topalli, K., Okyay, A.K.: Controlling luminescent silicon nanoparticle emission produced by nanosecond pulsed laser ablation: role of interface defect states and crystallinity phase. *RSC Adv.* **6**, 112520–112526 (2016). <https://doi.org/10.1039/C6RA24412B>
- Vaccaro, L., Sciortino, L., Messina, F., Buscarino, G., Agnello, S., Cannas, M.: Luminescent silicon nanocrystals produced by near-infrared nanosecond pulsed laser ablation in water. *Appl. Surf. Sci.* **302**, 62–65 (2014). <https://doi.org/10.1016/j.apsusc.2014.01.041>
- Wippermann, S., He, Y., Vörös, M., Galli, G.: Novel silicon phases and nanostructures for solar energy conversion. *Appl. Phys. Rev.* **3**, 040807 (2016). <https://doi.org/10.1063/1.4961724>
- Wu, C., Crouch, C.H., Zhao, L., Mazur, E.: Visible luminescence from silicon surfaces microstructured in air. *Appl. Phys. Lett.* **81**, 1999–2001 (2002)
- Yan, J.H., Liu, P., Lin, Z.Y., Wang, H., Chen, H.J., Wang, C.X., Yang, G.W.: Magnetically induced forward scattering at visible wavelengths in silicon nanosphere oligomers. *Nat. Commun.* **6**, 7042 (2015)
- Zaza, C., Violi, I.L., Gargiulo, J., Chiarelli, G., Schumacher, L., Jakobi, J., Olmos-Trigo, J., Cortes, E., König, M., Barcikowski, S., et al.: Size-selective optical printing of silicon nanoparticles through their dipolar magnetic resonance. *ACS Photon.* **6**, 815–822 (2019)

**Publisher's Note** Springer Nature remains neutral with regard to jurisdictional claims in published maps and institutional affiliations.

Springer Nature or its licensor (e.g. a society or other partner) holds exclusive rights to this article under a publishing agreement with the author(s) or other rightsholder(s); author self-archiving of the accepted manuscript version of this article is solely governed by the terms of such publishing agreement and applicable law.